Experimental Design and Field Validation of a 3DGS-based Rebar Inspection Testbed for Infrastructure Projects

Kumar Adarsh [1,2] Ashwani Jaiswal [1] and Nikhil Bugalia [1]

[1]Department of Civil Engineering, Indian Institute of Technology Madras, India
[2]Heavy Civil Infrastructure-IC, Larsen & Toubro Construction

ce23m111@smail.iitm.ac.in, ce22d045@smail.iitm.ac.in, nbugalia@civil.iitm.ac.in

Abstract -

Conventional rebar quality inspection in construction relies heavily on manual measurements, which are time-consuming, error-prone, and impractical for dense reinforcement layouts. 3D Gaussian Splatting (3DGS) has recently emerged as a promising technique for vision-based automated rebar inspection, enabling dense 3D reconstruction under complex reinforcement configurations. Despite this potential, most existing approaches lack systematic parameter optimization and are primarily validated under laboratory conditions, which limits their applicability and reliability on real-world construction sites. This study proposes a structured experimental design to identify optimal parameters for a 3DGS-based automated rebar inspection pipeline, thereby reducing the need for trial-and-error during on-site deployment. A key contribution of this work is the identification of an optimal parameter configuration, comprising 10–20k training steps, a maximum splat count of 1M, 1920p downsampling, and UHD recording resolution. These parameters are subsequently validated on real-world U-girder reinforcement cages captured under constrained site conditions. Among the five field datasets, three demonstrate reconstruction and detection performance consistent with simulated predictions. Field validation further confirms that elevated camera viewpoints significantly improve reconstruction completeness and rebar detectability. Overall, the proposed virtual testbed enables efficient pre-deployment optimization, reducing calibration effort and enhancing the robustness of 3DGS-based rebar inspection in real-world construction environments.

Keywords -

Rebar Inspection; Computer Vision; 3D Gaussian Splatting; Point Cloud; Optimization.

1 Introduction

In the construction industry, conventional quality assessment of reinforcement remains heavily reliant on manual inspection methods, which are both time-consuming and inconsistent, and introduce errors [1]. On-site engineers typically measure rebar spacing, alignment, and layout using tapes and gauges, which requires direct physical access to dense reinforcement cages. Such practices not only compromise inspection efficiency but may also disturb the reinforcement arrangement, affecting construction quality [2]. With increasing project complexity and workforce shortages, the conventional inspection method is becoming more challenging [3]. In this context, digital and automated vision-based rebar inspection systems have emerged as a more effective solution to overcome the limitations of conventional assessment, offering the potential to standardize assessments, reduce rework, and enable continuous monitoring of structural compliance.

An automated rebar inspection pipeline typically consists of two sequential key processes: (i) data acquisition and (ii) computational processing for quality assessment [1]. Data acquisition aims to capture geometric information of reinforcement cages. It has been implemented using various sensing modalities, such as terrestrial or mobile laser scanners (TLS/MLS), RGB-D cameras, or monocular RGB cameras [4]. TLS and MLS systems directly generate dense, accurate point clouds and have demonstrated high precision in rebar spacing measurements, particularly under laboratory conditions [2, 3]. However, these systems are costly, require skilled operators, and involve significant setup time, which limits their scalability for routine on-site deployment. RGB-D cameras offer a lower-cost alternative and can directly provide depth information, but their effective range and robustness remain constrained in cluttered or large-scale construction environments [5]. Consequently, monocular RGB cameras have attracted growing attention due to their low cost, ease of deployment, and flexibility in real construction settings.

Unlike TLS/MLS and RGB-D sensors, monocular RGB cameras do not directly produce 3D geometry; therefore, they require an additional 3D reconstruction or preprocessing step to recover spatial information. Traditionally, this reconstruction has been achieved using photogrammetry or multi-view stereo (MVS) techniques [6]. While MVS is computationally efficient and widely adopted, it often struggles to reliably reconstruct dense and repetitive geometries, such as closely spaced rebar cages, especially under occlusions and complex viewing conditions. These limitations significantly restrict the applicability of MVS-based pipelines in real-world rebar inspection scenarios.

Recently, 3-Dimensional Gaussian Splatting (3DGS) has emerged as a state-of-the-art technique for high-fidelity 3D reconstruction in visually complex scenes [7]. Compared to traditional MVS, 3DGS has demonstrated superior performance in handling repetitive patterns and complex occlusions. Recent studies have explored 3DGS-based rebar detection pipelines, typically developed and validated within a virtual reality (VR) environment, and have reported substantially improved geometric detail and reconstruction accuracy compared to MVS-based approaches [8]. However, the literature in this domain is nascent, is primarily focused on establishing a proof-of-concept experimental testbed, and does not systematically investigate the influence of 3DGS reconstruction parameter selection. Despite the demonstrated potential of 3DGS for reconstructing dense reinforcement geometries, its performance is susceptible to a range of reconstruction-level parameters [7, 9]. These parameters include the number of training steps, the maximum splat count, the image downsampling factor, and the selection of the best frames (training views). In addition, 3DGS performance is strongly influenced by field-level data acquisition parameters, such as the camera's trajectory, illumination levels, and recording resolution, which jointly affect view coverage and geometric quality [10]. However, existing studies employing 3DGS largely adopt fixed or empirically chosen parameter settings, without systematically examining their influence on reconstruction accuracy. This lack of parameter-level understanding represents a critical barrier to the reliable deployment of 3DGS-based rebar detection pipeline in real construction environments, where extensive trial-and-error optimization is impractical. Thus, there is a clear need for a structured experimental investigation that enables systematic parameter optimization prior to on-site deployment, thereby minimizing the effort required to tune and calibrate under real construction conditions.

Also, despite notable progress, the majority of existing automated rebar inspection studies are still evaluated primarily in laboratory or VR conditions. Among the reviewed literature, Yuan et al. (2023) present one of the few studies that conduct in-situ rebar inspection on a single-layer structural element, primarily focusing on relatively larger rebar spacing [2]. However, the study does not systematically account for variability in capture strategy, site constraints, or site conditions. In contrast, Kim et al. (2024) investigate multiple data collection scenarios to improve the generalizability of their approach [3]. However, their methodology is primarily validated in VR environments using synthetic datasets with single-layer rebar cages, and the framework lacks comprehensive validation on real-world data. More importantly, complex reinforcement geometries, such as multi-layered rebar cages in U-girders or I-girders, are underrepresented in existing field-based evaluations.

To address this research gap, this study builds upon a previously developed VR-based rebar inspection workflow featuring large-scale U-griders [8]. The study introduces a structured experimental design aimed at identifying optimal 3DGS reconstruction parameters (training steps, maximum splat count, image downsampling, and best frame selection). In parallel, key field-level data acquisition parameters (camera path, illumination, and recording resolution) are examined in the VR-based workflow to assess their impact on reconstruction quality. The resulting optimal data acquisition and reconstruction parameters are then field-validated on real on-site U-girders, where 3DGS-based rebar spacing measurements are compared with manual ground truth. The study makes significant contributions towards establishing systematic validation frameworks that bridge virtual (synthetic) or laboratory-based evaluations with real-world field validations.

2 Methodology

The methodology of this study builds upon the author's previous work on a 3DGS-based rebar detection pipeline. It extends it into a systematic framework for evaluating real-world scenarios and parameters to identify their optimal values.

2.1 3DGS-based Rebar Detection Pipeline

The developed pipeline follows a multi-step process. In the first stage, a synthetic environment is generated using the *Unity* engine, with a rebar cage designed in *Rhino* and a camera configuration to replicate realistic video capture conditions closely. The resulting environment is rendered as a video sequence and processed using *RealityCapture*. The synthetic video data are then processed using the 3DGS tool *Jawset PostShot* to generate splat cloud representations of the scene. These splat clouds are subsequently refined and denoised using *CloudCompare* to enhance data quality and remove outliers. Eventually, the cleaned point cloud is served as input to a custom analytical dashboard developed. Within this dashboard, K-means clustering is applied to segment the rebar into distinct layers, followed by a histogram-based projection method to identify individual rebar elements. Overall, this pipeline achieves a spacing error of less than 3% even for complex rebar configurations, such as U-girder (see

Figure 1). This end-to-end pipeline enables controlled experimentation while maintaining relevance to real-world conditions.

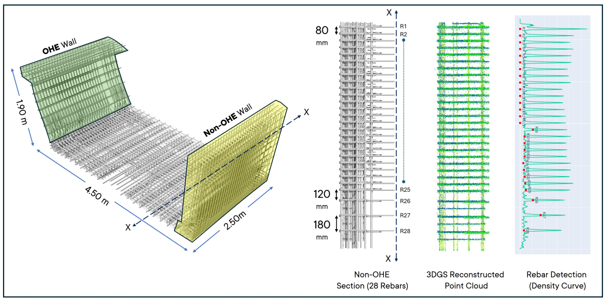

Figure 1. Overall process of rebar detection of non-OHE U-girder rebar cage.

2.2 Study Design and Evaluation Framework

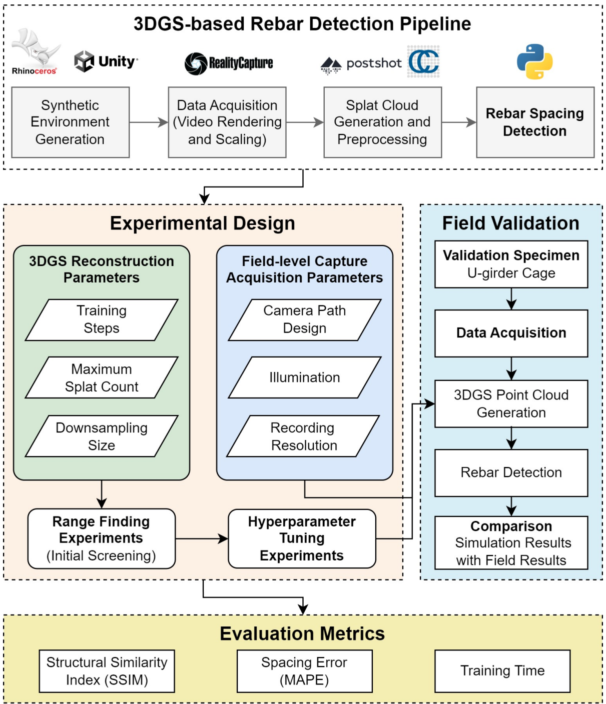

Figure 2. Schematic of the methodology of experimental design and field validation of the rebar detection pipeline.

The overall study design adopted in this research is illustrated in Figure 2. The study is structured into two main components: (i) controlled experiments conducted using synthetic data to investigate the influence of reconstruction and acquisition parameters, and (ii) field-level validation using real-world data captured from a representative U-girder specimen. To ensure consistent evaluation across all experiments and validation stages, a fixed region of interest within the U-girder rebar cage was selected as the reference layout (see Figure 1). The selected region corresponds to the non-OHE wall segment, which contains 28 closely spaced vertical rebars. This region was intentionally chosen for its high geometric complexity; the rebars are densely packed, partially occluded, and intersect with transverse reinforcement members, making both 3D reconstruction and rebar detection significantly more challenging than in single-layer rebar cage configurations.

3 Experimental Design

This section explains the experimental variables used to evaluate the 3DGS-based rebar inspection pipeline. The experiments were designed to separate reconstruction parameters from field-level acquisition parameters, enabling a systematic study of their individual and combined effects on inspection accuracy.

3.1 3DGS Reconstruction Parameters

The quality of 3DGS reconstruction is influenced by three key training parameters, namely training steps, maximum splat count, and downsampling size [7, 11]. These parameters were selected for systematic experimentation and varied individually using a one-factor-at-a-time approach, while all other conditions were kept constant. Specifically, during each experiment, a fixed orbital camera path, constant illumination (bright daylight), consistent recording resolution and identical preprocessing and reconstruction settings (other than the parameter under study) were maintained. **Training steps** control the duration of 3DGS optimization; increasing steps improves refinement of Gaussian position, shape, and colour up to a limit, beyond which gains are minimal and computation cost increases [11]. Hence, a range of training steps was tested to balance accuracy and efficiency. The **Maximum splat count** controls the number of Gaussian splats representing the scene. Higher values improve geometric detail for thin elements such as rebars but increase memory and training time; beyond a certain density, gains are marginal. Therefore, multiple splat limits were tested to identify a stable upper bound. Finally, the **Downsampling size** defines the resolution of input images during training. Higher resolutions preserve texture and edge detail but increase computational cost, so multiple levels were evaluated to determine the optimal setting. Range-finding experiments were conducted to establish suitable parameter bounds for subsequent hyperparameter tuning.

3.2 Field-level Data Acquisition Parameters

While 3DGS reconstruction parameters control the fidelity of the generated output, the overall rebar detection pipeline performance is also affected by field-level data-acquisition conditions. To investigate this effect, a series of systematic experiments was conducted. These experiments were carefully designed to identify optimal conditions for achieving efficient and reliable reconstruction and detection performance. Among the capture parameters, camera path design, illumination, and recording resolution were selected due to their direct impact on image quality, coverage, and reconstruction [9, 10, 11].

3.2.1 Camera Path Design

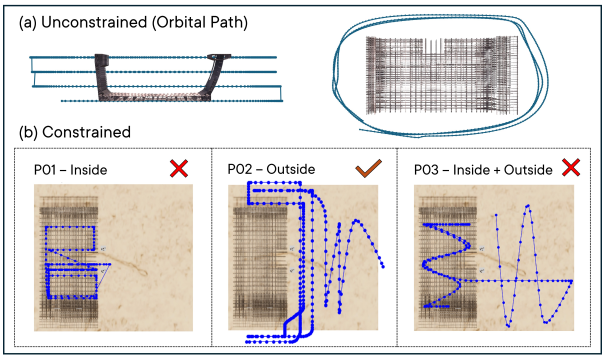

Figure 3. (a) Camera path design for unconstrained (orbital) and constrained scenarios (P01 to P03).

Camera path design determines how the camera moves around the rebar cage during data capture, directly influencing viewpoint diversity for reconstruction [10]. This experiment considers two practical site-based scenarios: unconstrained and constrained rebar cages. The unconstrained scenario represents cases where the rebar cage is fully accessible, allowing the camera to move and rotate freely around the structure. For this case, an orbital camera path was employed, in which the camera follows a closed-loop trajectory providing full 360° coverage of the cage at multiple fixed elevations. The constrained scenario reflects real construction conditions, where accessibility is limited, such as when rebar cages are embedded within U-girders or adjacent to formwork. To simulate these conditions, controlled camera paths were defined. Three configurations were evaluated: P01, where scanning is performed only from within the cage; P02, where scanning is performed only from outside the cage; and P03, which combines both inside and outside scanning. These paths were designed to assess the impact of accessibility constraints and camera placement on reconstruction performance.

3.2.2 Illumination

Illumination varies naturally throughout the day as the sun moves across the sky, resulting in fluctuations in on-site lighting conditions. For this reason, two illumination conditions were evaluated using experiments. First is a Bright daylight condition, representing typical outdoor precast yard environments, simulated at approximately 100,000 lux. Second is Low-light conditions, representing shaded or late-day site conditions, simulated at approximately 10,000 lux (see Figure 4a) [9].

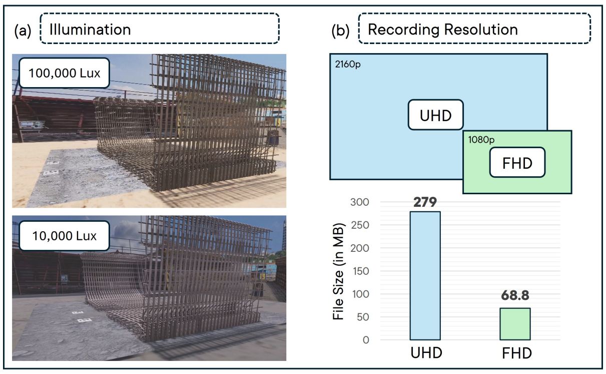

Figure 4. (a) Experimental variations for illumination, and (b) Recording resolution along with file size comparison.

3.2.3 Recording Resolution

The recording resolution of the raw video determines the finest pixel detail available before downsampling. Higher resolution offers more texture for feature matching, but at the expense of larger file sizes and longer processing times. The two most common recording resolutions were evaluated: FHD (1080p) and UHD (2160p) [12].

3.3 Evaluation Criteria

For evaluation purposes, an experiment was considered valid only if the rebar detection pipeline successfully detected all 28 rebars. Spacing errors were computed exclusively for these valid rebars using the Rhino model as ground truth. Three quantitative metrics were used consistently across all experiments to evaluate reconstruction quality, inspection accuracy, and computational feasibility. The first criterion is the Structural Similarity Index (SSIM). It captures similarity in structure, contrast, and luminance, and serves as an indicator of reconstruction stability rather than inspection accuracy. SSIM values were directly taken from *Jawset PostShot* after 3DGS reconstruction. The second criterion is Mean Absolute Percentage Error (MAPE), which measures the percentage deviation between detected rebar spacing values and the known ground-truth spacing obtained from the reference model, calculated using Equation (1).

$$\text{MAPE} = \frac{100}{n} \sum_{i=1}^{n} \frac{\left| e_i^T - e_i^P \right|}{e_i^T} \tag{1}$$

where n is the total number of spacings analysed in a trial. e_i^P denotes the spacing estimated by the workflow for the i-th bar pair, while e_i^T represents the corresponding ground-truth spacing obtained from manual calliper measurements (field data) or directly from the 3D model (synthetic data). The third evaluation criterion is training time, which represents the total duration required to complete the 3DGS reconstruction for a given configuration. This metric was recorded to evaluate the practical feasibility of the workflow and to balance accuracy gains against computational cost.

4 Results and Discussion

4.1 3DGS Reconstruction Parameters Results

This subsection discusses the influence of 3DGS generation parameters on reconstruction quality and spacing accuracy. The experiments were performed in two stages: range-finding and detailed hyperparameter tuning.

4.1.1 Range Finding Experiments

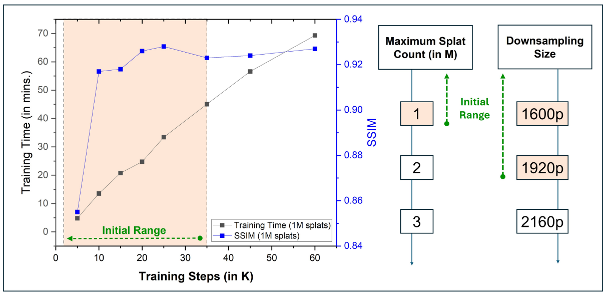

Figure 5. Training time and SSIM trends versus training steps, with highlighted initial range for maximum splat count and downsampling size.

Initially, a set of range-finding experiments was conducted to identify practical operating bounds for key 3DGS reconstruction parameters. A total of 19 experiments were performed using a fixed orbital camera path. Training steps varied from 5k to 60k, maximum splat count was set to 1M, 2M, and 3M, and input resolution was downsampled to 1600p, 1920p, and 2160p. Figure 5 illustrates the effect of training steps on SSIM and training time for a representative configuration (1M splats). While additional experiments with higher splat counts (2M and 3M) were conducted, they resulted in only marginal improvements in SSIM and no consistent reduction in MAPE. Therefore, these results are summarized here rather than explicitly plotted for clarity. Similarly, increasing the input resolution beyond 1920p results in higher training time, with negligible improvement in MAPE and only minor gains in SSIM, indicating diminishing returns beyond these thresholds.

4.1.2 Hyperparameter Tuning Experiments

Following the range-finding experiment, a structured hyperparameter tuning study was conducted to identify performance-efficient parameters for 3DGS reconstruction. A total of 60 experimental trials were conducted systematically by varying the reconstruction parameters listed in Table 1. The experimental results show a consistent trend across all resolutions. SSIM increases rapidly up to 20k training steps and plateaus thereafter for all resolutions (see Figure 6a). However, after reconstruction, the rebar detection pipeline with an 800p downsampling size failed to achieve complete rebar detection and was discarded (marked in red *). In addition, training with fewer than 10k training steps for resolutions 1600p and 1920p also failed. Thus, those samples were also discarded. The remaining samples demonstrated the best performance, achieving 100% rebar detection. Figure 6b compares the downsampling sizes of 1600p and 1920p, and for 1920p, the spacing error drops below 1% between 10k and 20k training steps.

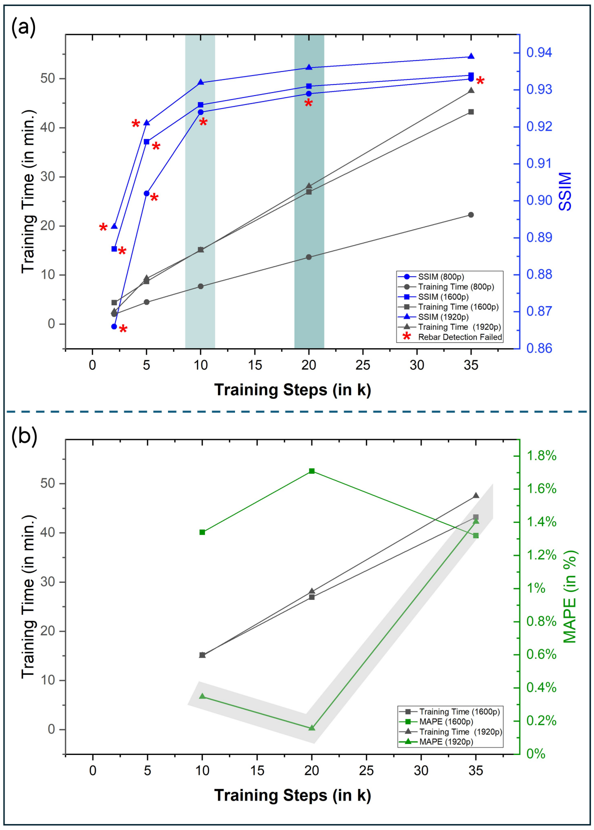

Figure 6. Training time versus training steps with SSIM, and (b) MAPE across different resolutions.

The maximum splat count strongly influenced detection reliability. Configurations with 0.1M and 0.2M splats frequently missed rebars, even at higher training steps. 0.5M splats improved detection but remained inconsistent, whereas 1M splats consistently achieved 100% rebar detection across valid configurations. Increasing splats beyond this value did not yield further accuracy gains. Overall, based on these observations, the hyperparameter tuning phase identified 10k -20k training steps, 1M maximum splats, and 1920p downsampling as the most optimal and computationally efficient configuration. These values were fixed for all subsequent site-level parameter experiments.

Table 1. Hyperparameter variations and total number of experiments

Hyperparameters	Variation	#
Training steps	2k / 5k / 10k / 20k / 35k	5
Maximum splats	0.1M / 0.2M / 0.5M / 1.0M	4
Downsampling size	800p / 1600p / 1920p	3
	Total Experiment	**60**

4.2 Field-Level Parameters Results

A total of 24 field-level experimental trials were conducted to evaluate the influence of capture conditions on reconstruction quality (SSIM) and spacing accuracy (MAPE). The experiments systematically varied camera trajectory, illumination level, and recording resolution, with reconstructions evaluated at training steps of 10k and 20k. Under controlled acquisition conditions, the orbital camera path consistently achieved 100% rebar detection and exhibited minimal spacing error. For constraint scenarios, only path P02 enabled complete rebar detection across all trials. Therefore, subsequent analysis for constraint scenarios is limited to the P02 path.

Under bright daylight conditions, the orbital camera path consistently achieved low spacing error, with MAPE values remaining below approximately 2% across most configurations (Figure 7a). In contrast, the P02 path exhibited slightly higher, yet stable, error levels (4%), indicating reduced sensitivity to training duration and resolution. A rebar detection failure was observed for the orbital trajectory at 20k training steps using FHD input, highlighting the limitations of lower-resolution capture even under favourable illumination.

Moderate daylight conditions resulted in substantially different behaviour (Figure 7b). While controlled-path MAPE remained relatively constant (2-3%), orbital-path reconstructions showed pronounced error inflation for FHD recordings, with MAPE exceeding 12% at both 10k and 20k training steps. This degradation was mitigated primarily by UHD capture, which consistently reduced spacing error to below 4%, thereby increasing robustness to illumination-related feature loss. Across both lighting conditions, recording resolution emerged as the dominant site-level factor. UHD recordings consistently outperformed FHD recordings in all scenarios, maintaining less than 4% MAPE across all experimental trials. Overall, the experimental results indicate that site-level parameters can significantly impact rebar inspection performance, even when reconstruction parameters are optimized. Another point is that increasing the training steps from 10k to 20k roughly doubled the training time but produced only a limited improvement in accuracy, indicating that recording resolution is more critical than deeper hyperparameter optimization for 3DGS reconstruction.

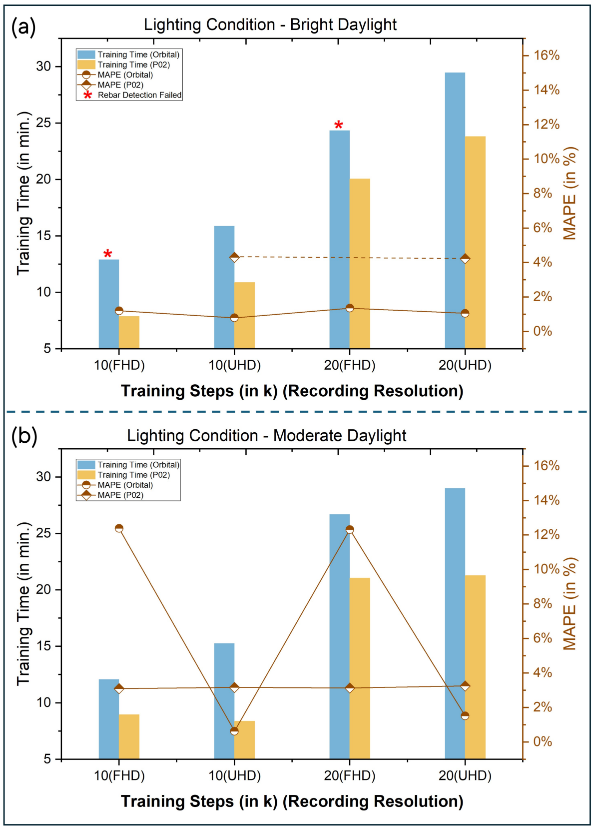

Figure 7. Training time and MAPE comparison for orbital and P02 camera path under (a) bright daylight. and (b) moderate daylight.

5 Site Validation

Site validation was conducted to verify whether the simulation-optimized parameters perform reliably under real-world precast yard conditions. A production U-girder reinforcement cage was evaluated under bright daylight, consistent with the simulated illumination setting.

5.1 Data Collection

For field validation, the capture strategies were intentionally designed to replicate the simulated strategies, including recording resolution, camera parameters, and

Table 2. Comparison across site validation, contrasting field data with its corresponding simulated data.

Trial	Recording Resolution	Training Steps (k)	Version	Training Time	SSIM	Detected Rebars (/28)	Detection Accuracy	MAPE (%)
1	FHD	10	S01	07:52	0.84	19	67.86%	–
			F01	10:25	0.65	27	96.43%	–
2	FHD	20	S02	20:03	0.87	23	82.14%	–
			F02	21:43	0.79	17	60.71%	–
3	UHD	10	S03	10:52	0.91	28	100.00%	4.31%
			F03	12:38	0.77	12	42.86%	–
4	UHD	20	S04	23:48	0.93	28	100.00%	4.23%
			F04	23:25	0.86	19	67.86%	–
			F04*	24:37	0.84	28	100.00%	15.03%

Note: S – Simulated, F – Field, F04* is data captured partially from the elevated ramp (shown in Figure 8b).

camera path. All recordings were captured from a smartphone device camera with fixed parameters across trials, matched to the simulation settings to ensure consistency with the underlying assumptions. Based on the experimental observations, both FHD and UHD recording resolutions, along with training steps of 10k and 20k, were selected, and the P02 camera path was fixed for data collection. All recordings were processed using the same multi-step rebar detection pipeline used in simulation. Evaluation was restricted to the same 28 rebars on the non-OHE wall to maintain consistency (See Figure 8a).

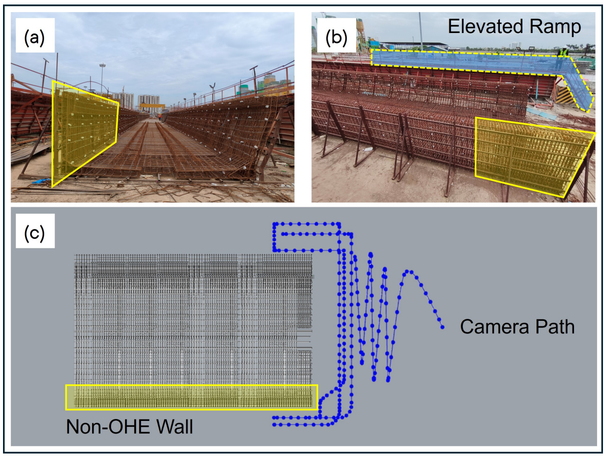

Figure 8. (a) U-girder reinforcement cage, (b) back-end isometric view highlighting elevated ramps, (c) schematic of the camera path used for site validation.

5.2 Field Validation Results

A total of five field samples were collected and processed using the rebar detection pipeline. The key parameters and their corresponding results are summarized in Table 2. Among the five samples, F01 and F02, captured in FHD resolution, failed to detect the rebars, identifying only 27 and 17 rebars, respectively. These results exactly match their corresponding simulated trials (S01 and S02), thereby classifying them as true negative cases. Although both cases resulted in incomplete detection, variations in detection accuracy between simulation and field trials indicate the influence of real-world factors, such as noise, illumination variability, and partial occlusions, that are not fully represented in the synthetic setup. Similarly, samples F03 and F04, which were captured in UHD, also failed to detect the rebars, detecting only 12 and 19 rebars, respectively. However, their replicated simulation cases (S03 and S04) were successful, classifying F03 and F04 as false positive cases.

In contrast to the four field trials that initially failed to achieve complete rebar detection, sample F04* was collected. The only variation in this case was that the capture was performed from a slightly elevated side view using an elevated ramp, as illustrated in Figure 8(b). In this sample, the rebar detection pipeline successfully detected all 28 rebars, with a MAPE of 15.03% in spacing estimation. Since the corresponding simulated case S04 also succeeded, this sample is considered a successful validation case and is treated as a true positive for outcome consistency, despite differences in capture geometry.

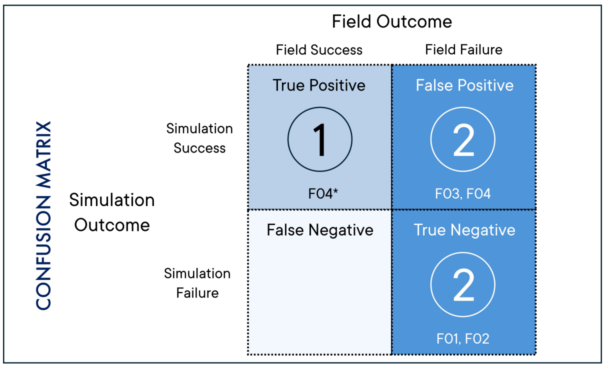

Figure 9. Confusion matrix summarizing agreement between simulation and field outcomes.

Figure 9 presents the confusion matrix derived from all evaluated samples. The key observations from the field trials indicate that under constrained scenarios, high-elevation capture is a decisive factor. Specifically, the introduction of a top-down perspective through elevated acquisition in F04* enabled complete rebar detection, confirming that at least one elevated camera pass is essential for successful reconstruction in dense reinforcement layouts, consistent with the role of viewpoint diversity in camera path design (Section 3.2.1). Additionally, spacing errors in the successful field sample (F04*) were higher than those observed in simulation (approximately 15%), reflecting the impact of real-world noise, material variability, and uncontrolled occlusions. Finally, the consistent failure of F01 and F02 in both field and simulation confirms that the simulation framework accurately identified capture geometries unsuitable for reliable reconstruction.

6 Conclusion

Existing studies on automated rebar spacing detection are largely limited to controlled environments or simple geometries, with limited focus on complex configurations, such as U-girders, and on real-world feasibility. This study addresses this gap by investigating a 3DGS-based inspection pipeline previously developed by the authors using a structured, simulation-driven experimental design [8]. The experimental results established practical limits for key 3DGS reconstruction parameters (10-20k training steps, 1M splat count, and downsampling size 1920p) beyond which accuracy gains diminish while computational cost increases. Further experiments demonstrated that site-level capture conditions, particularly the camera path design and UHD recording resolution, were critical. While orbital trajectories performed best under unconstrained conditions, constrained scenarios required carefully designed paths, with outside-only scanning (P02) being the most reliable.

Field validation of metro U-girders demonstrated general correspondence between simulated predictions and real-world performance, particularly in identifying both successful and failed inspection scenarios. However, variations observed between simulation and field results, including differences within failure cases and the influence of elevated camera viewpoints, indicate that these relationships are not yet fully characterized. In particular, while elevated camera viewpoints were observed to improve reconstruction completeness in constrained scenarios, this factor was not systematically explored within the synthetic virtual environment and therefore requires further investigation. Similarly, differences in detection accuracy between simulation and field trials highlight the impact of real-world conditions, such as noise, occlusions, and illumination variability, that are not fully captured in the synthetic environment. Overall, while the proposed framework demonstrates promising practical applicability, further validation across diverse capture conditions, elevated viewpoints, and site scenarios is required to strengthen generalizability.

References

[1] M.-K. Kim, J. P. P. Thedja, and Q. Wang. Automated dimensional quality assessment for formwork and rebar of reinforced concrete components using 3d point cloud data. *Automation in Construction*, 112:103077, April 2020. doi:10.1016/j.autcon.2020.103077.

[2] X. Yuan, A. Smith, R. Sarlo, C. D. Lippitt, and F. Moreu. Automatic evaluation of rebar spacing using lidar data. *Automation in Construction*, 131:103890, November 2021. doi:10.1016/j.autcon.2021.103890.

[3] B. Kim, S. P. K. R., Y. Natarajan, D. V, J. An, and D.-E. Lee. Real-time assessment of rebar intervals using a computer vision-based dvnet model for improved structural integrity. *Case Studies in Construction Materials*, 21:e03707, December 2024. doi:10.1016/j.cscm.2024.e03707.

[4] S. Li, B. Zhang, J. Zheng, D. Wang, and Z. Liu. Development of automated 3d lidar system for dimensional quality inspection of prefabricated concrete elements. *Sensors*, 24(23):7486, November 2024. doi:10.3390/s24237486.

[5] S. Wang, L. Deng, J. Guo, M. Liu, and R. Cao. Automatic quality inspection of rebar spacing using vision-based deep learning with rgbd camera. In *Proceedings of the 41st International Symposium on Automation and Robotics in Construction (ISARC)*, Lille, France, June 2024. doi:10.22260/ISARC2024/0009.

[6] A. H. Qureshi, W. S. Alaloul, A. Murtiyoso, S. J. Hussain, S. Saad, and M. A. Musarat. Smart rebar progress monitoring using 3d point cloud model. *Expert Systems with Applications*, 249:123562, September 2024. doi:10.1016/j.eswa.2024.123562.

[7] S. Liu, M. Yang, T. Xing, and R. Yang. A survey of 3d reconstruction: The evolution from multi-view geometry to nerf and 3dgs. *Sensors*, 25(18):5748, September 2025. doi:10.3390/s25185748.

[8] K. Adarsh, N. Bugalia, and A. Pal. Development of a vr-based testbed for automated rebar inspection in infrastructure projects. In *ASCE Construction Research Congress*, San Antonio, Texas, March 2026. Accepted.

[9] D. Rangelov, S. Waanders, K. Waanders, M. Van Keulen, and R. Miltchev. Three-dimensional reconstruction techniques and the impact of lighting conditions on reconstruction quality: A comprehensive review. *Lights*, 1 (1):1, July 2025. doi:10.3390/lights1010001.

[10] D. Rangelov, S. Waanders, K. Waanders, M. V. Keulen, and R. Miltchev. Impact of data capture methods on 3d reconstruction with gaussian splatting. *Journal of Imaging*, 11(2):65, February 2025. doi:10.3390/jimaging11020065.

[11] G. Grubert, F. Barthel, A. Hilsmann, and P. Eisert. Improving adaptive density control for 3d gaussian splatting. In *Proceedings of the 20th International Joint Conference on Computer Vision, Imaging and Computer Graphics Theory and Applications*, pages 610–621, Porto, Portugal, 2025. SCITEPRESS. doi:10.5220/0013308500003912.

[12] A. Jaiswal, N. Bugalia, and Q. Phuc Ha. Optimizing structure from motion parameters for volume estimation of construction and demolition waste. In *Proceedings of the 42nd International Symposium on Automation and Robotics in Construction (ISARC)*, Montreal, Canada, July 2025. doi:10.22260/ISARC2025/0127.